NJC

Accepted Manuscript

This article can be cited before page numbers have been issued, to do this please use: C. Kim, T. G. Jo, J. Lee, E. Nam, K. H. Bok and M. H. Lim, *New J. Chem.*, 2016, DOI: 10.1039/C6NJ01544A.

View Article Online
DOI: 10.1039/C6NJ01544A

A highly selective fluorescence sensor for Al^{3+} and CN^- in aqueous solution: biological applications and DFT calculations

Tae Geun Jo,[a] Jae Jun Lee,[a] Eunju Nam,[b] Kwon Hee Bok,[a] Mi Hee Lim,[b]* Cheal Kim*

[a]*Department of Fine Chemistry and Department of Interdisciplinary Bio IT Materials, Seoul National University of Science and Technology, Seoul 139-743, Republic of Korea. Fax: +82-2-973-9149; Tel: +82-2-970-6693; E-mail: chealkim@seoultech.ac.kr*

[b]*Department of Chemistry, Ulsan National Institute of Science and Technology (UNIST), Ulsan 44919, Republic of Korea. Fax: +82-52-217-5409; Tel: +82-52-217-5422; E-mail: mhlim@unist.ac.kr*

Abstract

A new "turn-on fluorescence type" chemosensor **1** (N'1,N'2-bis((E)-2-hydroxybenzylidene)oxalohydrazidehas) with a simple structure was devised and synthesized. In aqueous solution, the receptor **1** could efficiently detect both Al^{3+} and CN^- at two different wavelengths. The limit of detection for Al^{3+} (2.0 μM) is below the World Health Organization (WHO) guideline for drinking water (7.41 μM). To utilize a practical and biological application, the abilities of **1** for monitoring Al^{3+} were tested in real water samples and living cells. In addition, **1** showed a highly selective fluorescence enhancement for CN^- in the presence of other anions without any interference. The sensing mechanisms of **1** for Al^{3+} and CN^- were supported by theoretical calculations.

Keywords: Aluminium, Cyanide, Fluorescence sensor, Theoretical calculations, Cell imaging.

View Article Online
DOI: 10.1039/C6NJ01544A

1. Introduction

The development of highly sensitive and selective chemosensors for detecting metal ions and anions has always been of especial interest, because they play important roles in biological, chemical, ecological and endocrine systems.[1-5] These ions are also related to diverse environmental and health problems.[6-9] Therefore, qualitative and quantitative analysis of various ions have received considerable attention.[10-12] Among the various metal ions, Al^{3+} is the most abundant metal and the third most prevalent metallic elements in the earth's crust,[13,14] and its compounds are extensively used in chemical industry production, food additives, pharmaceuticals, water purification and industrial processes such as production of light alloys.[15] However, as a non-essential element in human body, Al^{3+} can be a competitive inhibitor of several essential elements, viz. Mg^{2+}, Ca^{2+} and Fe^{2+} due to its similarities in ionic size and charge.[16] Thus, the unregulated amounts of aluminium in the body may cause various problems, such as Al-related bone disease (ARBD), encephalopathy, myopathy, Parkinson disease and Alzheimer diseases.[17-19] The World Health Organization (WHO) has recommended the maximum limit of aluminium concentration to be at 200 μg L^{-1} (7.41 μM) in drinking water.[20] Therefore, it is important to develop accurate probes for detecting Al^{3+} because of its critical impact on human health. In fact, various sensors for Al^{3+} have been developed and reported[21-26] so far, but that there is still a lot of challenges, such as the sensing ability in aqueous solution.

Among the biologically and industrially crucial anions, cyanide has received the attention,[27-32] because it is well known as one of the most fatal toxic anions. Its toxicity is caused by its propensity to bind to the iron in cytochrome c oxidase, interfering with electron transport and resulting in hypoxia.[33-36] Despite these toxicities, various industrial processes such as raw materials for synthetic fibers, resins, herbicides, and the gold-extraction process require the presence of cyanide.[37,38] For this reason, considerable attention has been focused on developing reliable and efficient sensors for detecting the presence of cyanide.[39-42]

In particular, among various methods for detection of analytes, fluorescence technique, which has selective and sensitive ability of detecting important chemical species, is a very

View Article Online
DOI: 10.1039/C6NJ01544A

attractive research topic in the molecular imaging fields.[43-45] Therefore, fluorescence indicators have been extensively utilized as a versatile instrument in analytical chemistry, biochemistry, and cell imaging.[46-48]

The salicylidene Schiff bases can be easily synthesised by condensing of salicylaldehyde and amine derivatives,[49] and are known to be able to strongly bind the metal ions, resulting in different optical properties according to a type of the metal ions.[50-54] In addition, Schiff bases containing phenolic groups are sometimes used as sensors for anions because of the ability of the phenolic-OH group to interact with anions through hydrogen bonding even in aqueous solution.[55-60] Considering this facts, we designed **1** as a dual-target sensor that could strongly coordinate to metal ions through Schiff base (imine) and interact with the targeted anions through hydrogen bond of the phenolic-OH groups.

Herein, we report synthesis, characterization, and sensing properties of the chemosensor **1** for Al^{3+} and CN^- which was based on the combination of 2-hydroxybenzaldehyde and oxalohydrazide. **1** showed a selective enhancement of fluorescence in the presence of Al^{3+} ions in a near-perfect aqueous solution. In particular, **1** could be used to detect Al^{3+} in real water samples and biological systems. In addition, **1** could also detect CN^- by fluorescence enhancement among various ions in aqueous media. Moreover, the sensing mechanisms for the detection of Al^{3+} and CN^- were proposed and supported by the theoretical calculation methods.

2. Experimental

2.1 Reagents and apparatus

Unless otherwise specified, all the solvents and reagents (analytical grade and spectroscopic grade) were obtained commercially and used without further purification. ^1H NMR and ^{13}C NMR measurements were performed on a Varian 400 MHz and 100 MHz spectrometer and chemical shifts (δ) were recorded in ppm. Absorption spectra were recorded at 25℃ using a Perkin Elmer model Lambda 25 UV/Vis spectrometer. Electrospray ionization mass spectra (ESI-mass) were collected on a Thermo Finnigan (San

View Article Online
DOI: 10.1039/C6NJ01544A

Jose, CA, USA) LCQ^{TM} Advantage MAX quadrupole ion trap instrument. The spray voltage was set at 4.2 kV, and the capillary temperature was set at 80 ℃. Elemental analysis for carbon, nitrogen, and hydrogen was carried out by using a Flash EA 1112 elemental analyzer (thermo) in Organic Chemistry Research Center of Sogang University, Korea.

2.2 Synthesis of receptor 1

A solution of 2-hydroxybenzaldehyde (0.98 g, 8.0 mmol) was added to a solution containing oxalohydrazide (0.12 g, 2.0 mmol) in methanol, followed by addition of three drops of phosphoric acid into the reaction mixture. The reaction mixture was stirred for 3 d at room temperature. A white precipitate produced was collected by filtration, washed several times with methanol, and dried in a vacuum to obtain the pure white solid. The yield was 75.4%. ^{1}H NMR (400 MHz, DMSO-d_6) δ: 12.60 (s, 2H), 10.98 (s, 2H), 8.81 (s, 2H), 7.54 (d, 2H), 7.32 (t, 2H), 6.92 (m, 4H); ^{13}C NMR (100 MHz, DMSO-d_6, ppm): 157.50, 155.75, 151.13, 131.86, 129.34, 119.32, 118.48, 116.36 ppm. ESI-MS m/z [**1**-H$^+$]$^-$: calcd, 325.09, found, 325.10. Anal. Calcd for $C_{16}H_{14}N_4O_4$ (M.W. = 326.10): C, 58.90; H, 4.32; N, 17.17 %. Found: C, 58.85; H, 4.43; N, 17.12 %.

2.3 Fluorescence titraions of 1

For Al^{3+}; sensor **1** (0.5 mg, 0.0015 mmol) was dissolved in DMSO (0.5 mL) and 5 μL of the sensor **1** (3 mM) was diluted to 2.995 mL with bis-tris buffer solution (10 mM, pH 7.0) to make the final concentration of 5 μM. $Al(NO_3)_3$ (0.10 mmol) was dissolved in bis-tris buffer (5 mL) and 3.0-48.0 μL of the Al^{3+} ion solutions (20 mM) were added to the solution of **1** (5 μM) prepared above. After mixing them for a few seconds, fluorescence spectra were taken at room temperature.

For CN^-; sensor **1** (0.5 mg, 0.0015 mmol) was dissolved in DMSO (0.5 mL) and 30 μL of the sensor **1** (3 mM) was diluted to 2.97 mL with bis-tris buffer/DMSO (1/1, v/v) to make a final concentration of 30 μM. Tetraethylammonium cyanide (TEACN, 0.2 mmol) was dissolved in bis-tris buffer (5 mL) and 3.6-72.0 μL of the CN^- solutions (100 mM) were added to the solution of **1** (30 μM) prepared above. After mixing them for a few seconds, fluorescence spectra were taken at room temperature.

View Article Online
DOI: 10.1039/C6NJ01544A

2.4 UV-vis titrations of 1

For Al^{3+}; sensor **1** (0.5 mg, 0.0015 mmol) was dissolved in DMSO (0.5 mL) and 40 μL of the sensor **1** (3 mM) was diluted to 2.96 mL with bis-tris buffer solution (10 mM, pH 7.0) to make the final concentration of 40 μM. $Al(NO_3)_3$ (0.5 mmol) was dissolved in bis-tris buffer (5 mL) and 4.8-57.6 μL of the Al^{3+} ion solutions (100 mM) were transferred to the solution of **1** (40 μM) prepared above. After mixing them for a few seconds, UV-vis spectra were taken at room temperature.

For CN^-; sensor **1** (0.5 mg, 0.0015 mmol) was dissolved in DMSO (0.5 mL) and 30 μL of the sensor **1** (3 mM) was diluted to 2.97 mL with bis-tris buffer/DMSO (1/1, v/v) to make a final concentration of 30 μM. TEACN (1.0 mmol) was dissolved in bis-tris buffer (5 mL) and 18-144 μL of the CN^- solutions (200 mM) were transferred to the solution of **1** (30 μM) prepared above. After mixing them for a few seconds, UV-vis spectra were taken at room temperature.

2.5 Job plot measurements

For Al^{3+}; sensor **1** (0.5 mg, 0.0015 mmol) was dissolved in DMSO (0.5 mL) and 1.0 mL of the sensor **1** (3 mM) was diluted to 29.0 mL with bis-tris buffer solution (10 mM, pH 7.0) to make the final concentration of 100 μM. 5.0, 4.5, 4.0, 3.5, 3.0, 2.5, 2.0, 1.5, 1.0, 0.5 and 0 mL of the receptor **1** solutions were taken and transferred to vials. In the same way, $Al(NO_3)_3$ (0.1 mmol) was dissolved in bis-tris buffer (1 mL) and 0.03 mL of the Al^{3+} solution was diluted to 29.97 mL of bis-tris buffer solution (10 mM bis-tris, pH 7.0) to make the concentraiton of 100 μM. 0, 0.5, 1.0, 1.5, 2.0, 2.5, 3.0, 3.5, 4.0, 4.5 and 5.0 mL of the Al^{3+} solutions were added to each diluted **1** solution, seperately. Each vial had a total volume of 5 mL. After shaking them for a few seconds, UV-vis spectra were taken at room temperature.

For CN^-; sensor **1** (0.5 mg, 0.0015 mmol) was dissolved in DMSO (0.5 mL) and 1 mL of the sensor **1** (3 mM) was diluted to 29.0 mL with bis-tris buffer/DMSO (1/1, v/v) to make the final concentration of 100 μM. 5.0, 4.5, 4.0, 3.5, 3.0, 2.5, 2.0, 1.5, 1.0, 0.5 and 0 mL of the receptor **1** solutions were taken and transferred to vials. In the same way, TEACN

View Article Online
DOI: 10.1039/C6NJ01544A

(0.01 mmol) was dissolved in bis-tris buffer (1 mL) and 0.3 mL of the CN^- solution was diluted to 29.7 mL with bis-tris buffer/DMSO (1/1, v/v) to make the concentraiton of 100 μM. 0, 0.5, 1.0, 1.5, 2.0, 2.5, 3.0, 3.5, 4.0, 4.5 and 5.0 mL of the CN^- solutions were added to each diluted **1** solution, seperately. Each vial had a total volume of 5 mL. After shaking them for a few seconds, fluorescence spectra were taken at room temperature.

2.6 Competition with other metal ions or anions

For Al^{3+}; sensor **1** (0.5 mg, 0.0015 mmol) was dissolved in DMSO (0.5mL) and 5 μL of the sensor **1** (3 mM) was diluted to 2.995 mL with bis-tris buffer solution (10 mM, pH 7.0) to make the final concentration of 5 μM. MNO_3 (M = Na, K, 0.02 mmol) or $M(NO_3)_2$ (M = Mn, Co, Ni, Cu, Zn, Cd, Mg, Ca, Pb, 0.02 mmol) or $M(NO_3)_3$ (M = Fe, Cr, Al, Ga, In, 0.02 mmol) or $M(ClO_4)_2$ (M = Fe, 0.02 mmol) was dissolved in bis-tris buffer (1 mL). 39.0 μL of each metal solution (20 mM) was taken and added to 3 mL of the solution of receptor **1** (5 μM) to give 52 equiv. Then, 39.0 μL of Al^{3+} solution (20 mM) was added to the mixed solutions of each metal ion and **1** to make 52 equiv. After mixing them for a few seconds, fluorescence spectra were obtained at room temperature.

For CN^-; sensor **1** (0.5 mg, 0.0015 mmol) was dissolved in DMSO (0.5 mL) and 30 μL of the sensor **1** (3 mM) was diluted to 2.97 mL with bis-tris buffer/DMSO (1/1, v/v) to make a final concentration of 30 μM. Stock solutions (100 mM) of the tetraethylammonium salts of F^-, CN^-, Cl^-, Br^- and I^-, the tetrabutylammonium salts of AcO^-, $H_2PO_4^-$, BzO^-, N_3^- and SCN^-, and NaSH were separately dissolved in bis-tris buffer (1 mL). 64.8 μL of each anion solution (100 mM) was taken and added to 2.94 mL of the solution of receptor **1** (30 μM) to give 72 equiv. Then, 64.8 μL of TEACN solution (30 mM) was added to the mixed solutions of each anion and **1** to make 72 equiv. After mixing them for a few seconds, fluorescence spectra were obtained at room temperature.

2.7 pH effect test

A series of buffers with pH values ranging from 2 to 12 was prepared by mixing sodium hydroxide solution and hydrochloric acid in bis-tris buffer.

View Article Online
DOI: 10.1039/C6NJ01544A

For Al^{3+}; after the solution with a desired pH was achieved, sensor **1** (0.5 mg, 0.0015 mmol) was dissolved in DMSO (0.5 mL), and 5 μL solution of the sensor **1** (3 mM) was diluted to 2.995 mL with bis-tris buffer (10 mM, pH 7.0) to make the final concentration of 5 μM. $Al(NO_3)_3$ (0.10 mmol) was dissolved in bis-tris buffer (5 mL) and 39.0 μL of the Al^{3+} ion solution (20 mM) was added to the solution of **1** (5 μM) prepared above. After mixing them for a few seconds, fluorescence spectra were taken at room temperature.

For CN^-; after the solution with a desired pH was achieved, sensor **1** (0.5 mg, 0.0015 mmol) was dissolved in DMSO (0.5 mL), and 30 μL solution of the sensor **1** (3 mM) was diluted to 2.97 mL with bis-tris buffer/DMSO (1/1, v/v) to make the final concentration of 30 μM. TEACN (0.10 mmol) was dissolved in bis-tris buffer (1 mL) and 64.8 μL of the TEACN ion solution (100 mM) was added to the solution of **1** (30 μM) prepared above. After mixing them for a few seconds, fluorescence spectra were taken at room temperature.

2.8 Determination of Al^{3+} in water samples

Fluorescence spectral measurements of water samples containing Al^{3+} were carried by adding 15 μL solution of the sensor **1** (3 mM) and 0.60 mL of 50 mM bis-tris buffer stock solution to 2.385 mL sample solutions. After mixing them for a few seconds, fluorescence spectra were taken at room temperature.

2.9 Imaging experiments in living cells

HeLa cells (ATCC, Manassas, USA) were maintained in media containing DMEM, 10% fetal bovine serum (FBS, GIBCO, Grand Island, NY, USA), 100 U/mL penicillin (GIBCO), and 100 mg/mL streptomycin (GIBCO). The cells were grown in a humidified atmosphere with 5 % CO_2 at 37 ℃. Cells were seeded onto confocal imaging dish (SPL Life Sciences Co., Ltd., South Korea) at a density of 150,000 cells per 1 mL and then incubated at 37 ℃ for 24 h. Cells were first stained with SYTO16 nucleic acid stain (0.5 % v/v final DMSO concentration; 2.5 μM; at 37 ℃) for 20 min. Prior to addition of aluminum nitrate (dissolved in water), cells were washed with 2 mL of 10 mM bis-tris buffer (pH 7.4, 150 mM NaCl). After incubation with aluminum nitrate for 1 h, cells were exposed to **1** (dissolved in DMSO; 1% v/v final DMSO concentration; 20 μM; at room temperature) for

View Article Online
DOI: 10.1039/C6NJ01544A

30 min. Imaging was performed with an EVOS FL fluorescence microscope (Life technologies) using a DAPI light cube (DAPI, 2-(4-amidinophenyl)-1*H*-indole-6-carboxamidine; λ_{ex} = 357 (± 22) nm; λ_{em} = 447 (± 30) nm) and GFP light cube (λ_{ex} = 470 (±11) nm; λ_{em} = 510 (±21) nm).

2.10 ^{1}H NMR titrations

For ^{1}H NMR titrations of receptor **1** with Al^{3+}, three NMR tubes of receptor **1** (3.3 mg, 0.01 mmol) dissolved in DMSO-d_6 were prepared and then three different concentrations (0, 0.005 and 0.01 mmol) of $Al(NO_3)_3$ dissolved in DMSO-d_6 were added to each solution of receptor **1**. After shaking them for a minute, ^{1}H NMR spectra were taken at room temperature.

For ^{1}H NMR titrations of receptor **1** with CN^-, four NMR tubes of receptor **1** (3.3 mg, 0.01 mmol) dissolved in DMSO-d_6 were prepared and then four different concentrations (0, 0.005, 0.01 and 0.02 mmol) of TEACN dissolved in DMSO-d_6 were added to each solution of receptor **1**. After shaking them for a minute, ^{1}H NMR spectra were taken at room temperature.

2.11 Theoretical calculations

All theoretical calculations were performed by using the Gaussian 03 suite.[61] The singlet ground states (S_0) were optimized by DFT methods with Becke's three parametrized Lee-Yang-Parr (B3LYP) exchange functional[62,63] with 6-31G** basis set[64,65]. In vibrational frequency calculations, there was no imaginary frequency, suggesting that the optimized structures represented local minima. To investigate the electronic properties of singlet excited states, time-dependent DFT (TD-DFT) was performed in the ground state geometries. The Cossi and Barone's CPCM (conductor-like polarizable continuum model)[66,67] was used to consider the solvent effect. The 20 singlet-singlet excitations were calculated and analyzed. The GaussSum 2.1[68] was used to calculate the contributions of molecular orbitals in electronic transitions.

View Article Online
DOI: 10.1039/C6NJ01544A

3. Results and discussion

The compound **1** was obtained by the coupling reaction of 2-hydroxybenzaldehyde and oxalohydrazide with a 75.4% yield in methanol (Scheme 1) and characterized by ^{1}H NMR and ^{13}C NMR, ESI-mass spectrometry, and elemental analysis.

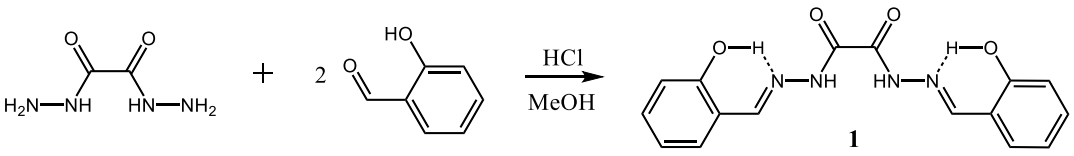

Scheme 1. Synthesis of sensor **1**.

3.1 Fluorescence and absorption studies of 1 toward Al^{3+}

The fluorescence selectivity of sensor **1** toward various metal ions was investigated in bis-tris buffer solution (10 mM, pH 7.0). Upon excitation at 410 nm, **1** exhibited a weak emission intensity at 488 nm with a low quantum yield (Φ = 0.011) (Fig. 1). Upon the addition of 52 equiv of metal ions (Al^{3+}, Ga^{3+}, In^{3+}, Zn^{2+}, Cd^{2+}, Cu^{2+}, Fe^{2+}, Fe^{3+}, Mg^{2+}, Cr^{3+}, Co^{2+}, Ni^{2+}, Na^{+}, K^{+}, Ca^{2+}, Mn^{2}, Pb^{2+}), only Al^{3+} induced a significant fluorescence enhancement at 491 nm with a quantum yield (Φ = 0.120), while other metal ions showed no obvious change in the spectra. The enhancement of fluorescence intensity could be explained by chelation-enhanced fluorescence (CHEF). The formation of a chelate complex between **1** and Al^{3+} might cause a rigid system, leading to CHEF effect (Scheme 2).[69-72]

View Article Online
DOI: 10.1039/C6NJ01544A

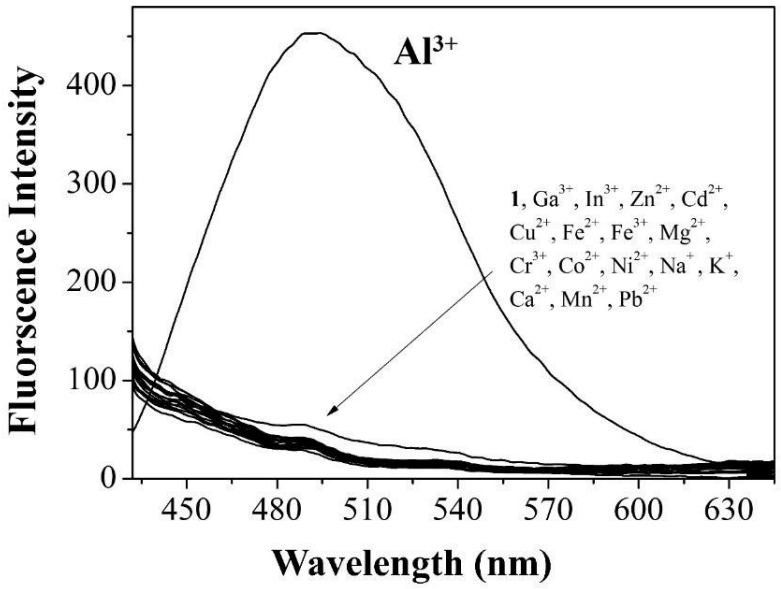

Fig. 1 Fluorescence spectral changes of **1** (5 μM) in the presence of different metal ions (52 equiv) such as Ga^{3+}, In^{3+}, Zn^{2+}, Cd^{2+}, Cu^{2+}, Fe^{2+}, Fe^{3+}, Mg^{2+}, Cr^{3+}, Co^{2+}, Ni^{2+}, Na^{+}, K^{+}, Ca^{2+}, Mn^{2+} and Pb^{2+} with an excitation of 410 nm in bis-tris buffer solution.

To study a quantitative investigation for the binding affinity of **1** with Al^{3+}, a fluorescence titration experiment of **1** was performed with Al^{3+} ion (Fig. 2). Upon the addition of Al^{3+} into **1**, the emission intensity at 491 nm steadily increased until the amount of Al^{3+} reached 52 equiv. Moreover, UV-vis titration experiment of **1** was conducted. The addition of Al^{3+} to a solution of **1** showed that the absorption bands at 298 nm and 475 nm decreased and a new band at 399 nm increased gradually until the amount of Al^{3+} reached 48 equiv (Fig. 3). Two isosbestic points were observed at 367 nm and 448 nm, suggesting that only one product was generated from **1** upon binding to Al^{3+}.

View Article Online
DOI: 10.1039/C6NJ01544A

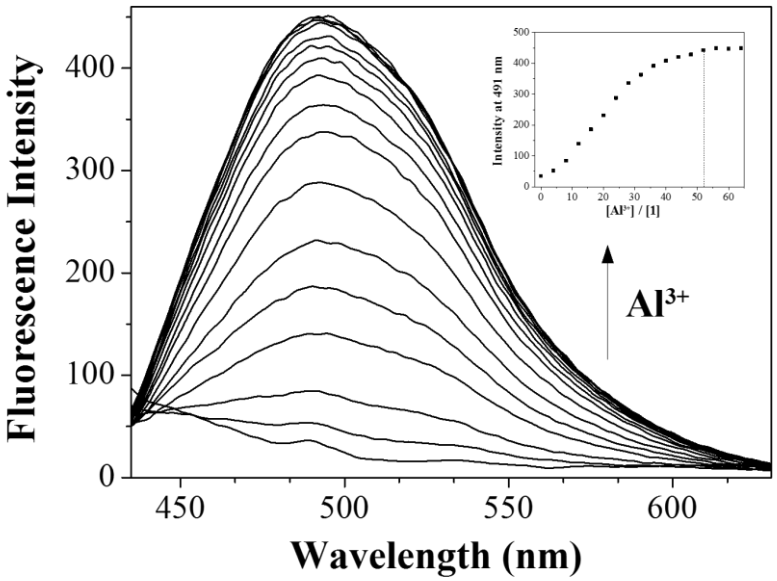

Fig. 2 Fluorescence spectral changes of **1** (5 μM) in the presence of different concentrations of Al^{3+} ions in bis-tris buffer solution. Inset: intensity (at 491 nm) of **1** as a function of Al^{3+} equiv.

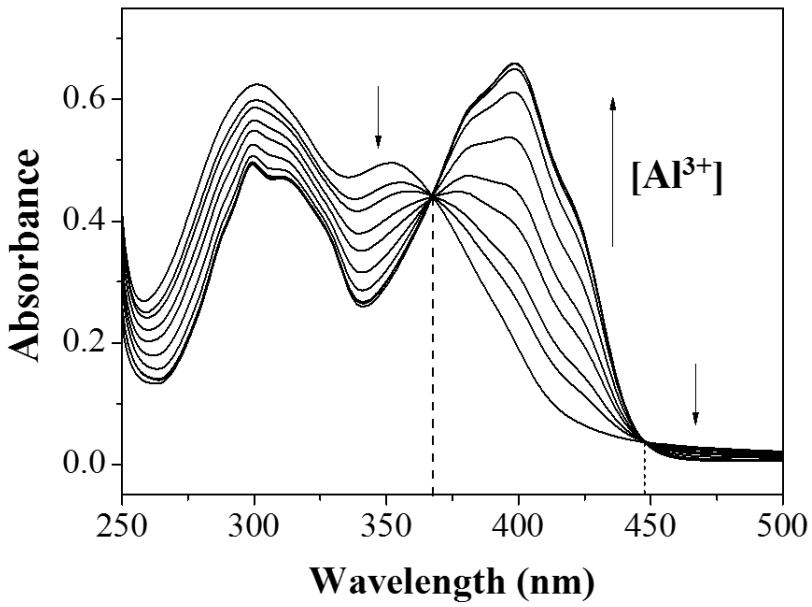

View Article Online
DOI: 10.1039/C6NJ01544A

Fig. 3 UV-vis absorption spectra of **1** (30 μM) obtained during the titration with $Al(NO_3)_3$ (0.12-1.92 mM) in bis-tris buffer solution.

The Job plot[73] referred to a 1:1 complexation stoichiometry between **1** and Al^{3+} (Fig. S1), which was further confirmed by ESI-mass spectrometry analysis (Fig. S2). The positive mass spectrum indicated that the first major peak at m/z = 424.10 was assignable to **1**-Al^{3+} complex - 2H + DMF [calcd, m/z: 424.10] and the second major peak at m/z = 351.00 was assignable to **1**-Al^{3+} complex- 2H [calcd, m/z: 351.07]. From the fluorescence titration, the association constant (*K*) of the **1**-Al^{3+} complex was determined as 4.0×10^3 M^{-1} through Benesi-Hildebrand equation (Fig. S3), which is within the range of those (10^3~10^9) previously reported for Al^{3+} binding chemosensors.[74-77] The detection limit[78] of receptor **1** as a fluorescence sensor for the analysis of Al^{3+} ions was found to be 2.01 μM (Fig. S4). The detection limit was below the WHO guideline for drinking water (7.41 μM), which indicated that **1** could be a practical detector of aluminum ions in drinking water.

The preferential selectivity of **1** for the detection of Al^{3+} was studied in the presence of other competitive metal ions of the same concentration (Fig. S5). In the presence of Ga^{3+}, In^{3+}, Zn^{2+}, Cd^{2+}, Mg^{2+}, Na^{+}, K^{+}, Ca^{2+}, Mn^{2+}, and Pb^{2+}, there was no obvious interference with the detection of Al^{3+}, while relatively high interferences were observed in the presence of Cu^{2+}, Fe^{2+}, Fe^{3+}, Co^{2+}, Ni^{2+} and Cr^{3+}. Nevertheless, it is worth noting that In^{3+} and Ga^{3+} hardly inhibited the fluorescence intensity of the **1**-Al^{3+} complex, while it has been a challenge to distinguish Al^{3+} from In^{3+} and Ga^{3+} due to the similar properties of all three ions.[79-81] To further check the preferential selectivity of **1** toward Al^{3+} in the presence of CN^-, the competitive study was carried out in bis-tris buffer solution. As shown in Fig. S6, no interference was observed with CN^- under the condition.

The sensing ability at biologically relevant pH is important for the practicality of the sensor. Thus, we conducted pH effect test in the pH range of 2 to 12 (Fig. S7). The stable and strong fluorescence intensity of **1**-Al^{3+} complex remained between pH 4 and 10. These results indicated that sensor **1** could be a good detector over a wide range of pH.

View Article Online
DOI: 10.1039/C6NJ01544A

In order to examine the applicability of **1** in real samples, we carried out the construction of a calibration curve for quantitative determination of Al^{3+} by **1** (Fig. S8). Receptor **1** exhibited a good linear relationship between the absorbance of **1** and the Al^{3+} concentration (0.0-70.0 μM) with a correlation coefficient of $R^2 = 0.9918$ (n = 3). This result indicates that **1** could be appropriate for the quantitative analysis of Al^{3+}. Based on the calibration curve, the chemosensor **1** was applied for the determination of Al^{3+} in the tap and drinking water samples (Table 1). The satisfactory recoveries and R.S.D. values were obtained.

Table 1. Determination of Al^{3+} in water samples[a]

Sample	Al^{3+} added (μmol/L)	Al^{3+} found (μmol/L)	Recovery (%)	R.S.D. (n = 3) (%)
Tap water	0.00	0.00	-	-
	40.0	38.2	98.2	0.6
Drinking water	0.00	0.00	-	-
	40.0	37.4	97.6	1.7

[a] Conditions: [**1**] = 15 μmol/L in 10 mM bis-tris buffer solution (pH 7.0).

In light of the above favorable spectroscopic properties of **1** for detecting Al^{3+}, including high selectivity, high sensitivity and rapid response in the physiological pH range, we studied its utility for monitoring Al^{3+} in biological systems. Cells were treated with Al^{3+} for 1 h and then **1** was added into them (Fig. 4). The background fluorescence was not observed in the cells that had not been exposed to Al^{3+}. Compared to the unexposed cells, discernible fluorescence could be observed in the cells exposed to Al^{3+} (100 μM). These observations confirm that **1** can be a potential detector to successfully sense Al^{3+} in biological systems. Furthermore, to identify the fluorescent localization in cells, the nuclei of cells were stained

View Article Online
DOI: 10.1039/C6NJ01544A

with SYTO16. As shown in Fig. 4e and f, the overlapped fluorescent images between **1**-Al^{3+} and SYTO16 suggested that the fluorescence response of **1** to Al^{3+} occurred in the overall parts of cells, including nuclei and cytoplasms.

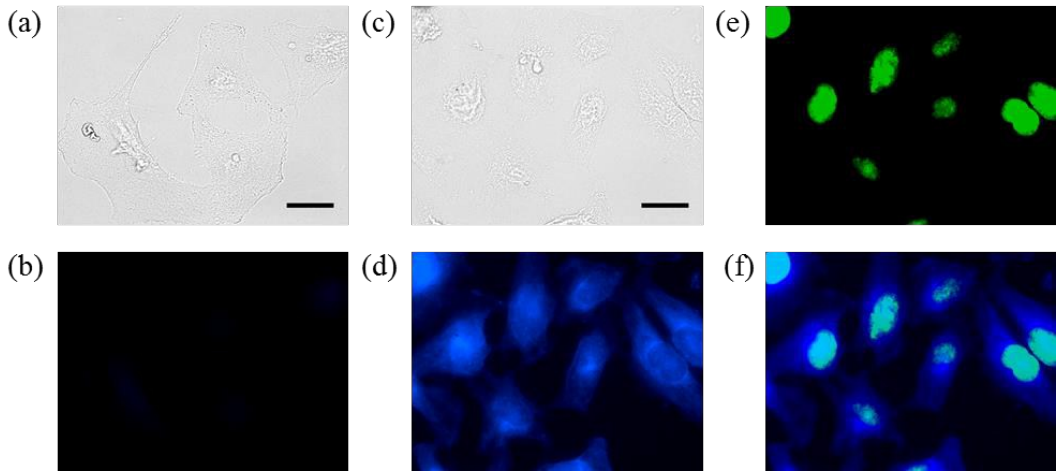

Fig. 4 Fluorescent response to Al^{3+} in the presence of **1** in HeLa cells. Cells were exposed to (a, b) 0 or (c-f) 100 μM Al^{3+} for 1 h prior to addition of **1** (20 μM). (a, c) Bright-field images of cells without or with Al^{3+}, respectively. Fluorescent responses to Al^{3+} were detected by **1** in the (b) absence or (d) presence of Al^{3+}. To investigate the distribution of fluorescence, (e) nuclei of cells were stained with SYTO16 (2.5 μM). (f) Overlapped fluorescence of (d) and (e). Conditions: DAPI channel [λ_{ex} = 357 (± 22) nm; λ_{em} = 447 (± 30) nm] for (b) and (d); GFP channel [λ_{ex} = 470 (± 11) nm; λ_{em} = 510 (± 21) nm] for (e). The scale bar is 25 μm.

We have performed ^1H NMR titrations to further examine the binding mode of **1** with Al^{3+} (Fig. S9). Upon addition of Al^{3+}, the proton H_1 almost disappeared, and the rest protons, H_2, H_3, H_4, H_5, H_6 and H_7, showed slightly down-field shifts. These results suggest that the two nitrogen atoms of the amide moieties might coordinate to Al^{3+} ion. There was no shift in the position of proton signals on further addition of Al^{3+} (>1.0 equiv), which indicates a

View Article Online
DOI: 10.1039/C6NJ01544A

1:1 binding of **1** to Al^{3+}. Based on Job plot, ESI-mass spectrometry analysis, and ^1H NMR titration, we proposed the structure of **1**-Al^{3+}complex (Scheme 2).

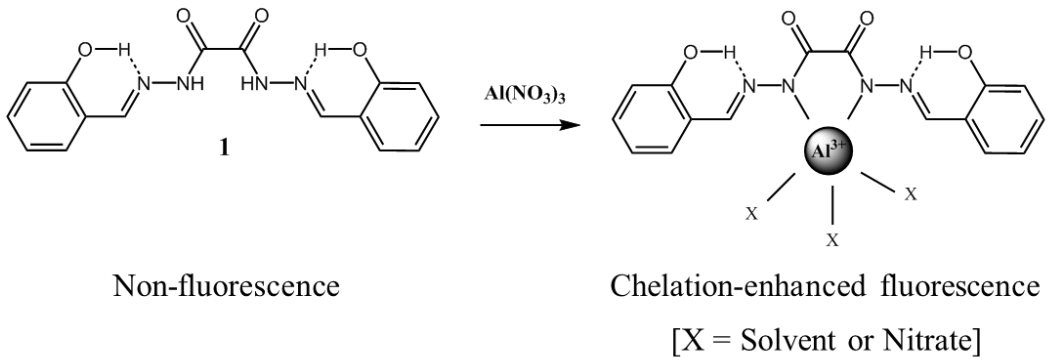

Scheme 2. Fluorescence enhancement mechanism and proposed structure of **1**-Al^{3+} complex.

To clearly understand the fluorescent sensing mechanism of **1** toward Al^{3+}, geometric optimizations were conducted for **1** and **1**-Al^{3+} complex by applying the B3LYP/6-31g** with CPCM/water, based on Job plot, ESI-mass spectrometry analysis and ^1H NMR titration (Fig. 5). The energy-minimized structure of **1** showed a distorted structure with the dihedral angle of 2N, 3C, 4C, 5N = 44.659º (Fig. 5a). **1**-Al^{3+} complex has a planar structure with the dihedral angle of 2N, 3C, 4C, 5N = 0º, and Al^{3+} was coordinated to 2N and 5N atoms of **1** (Fig. 5b). We further investigated the singlet excitations of **1** and **1**-Al^{3+} complex by TD-DFT methods and compared the UV-vis spectra of **1** and **1**-Al^{3+} with their TD-DFT calculations (Figs. S10a and S11a). In case of **1**, the main molecular orbital (MO) contributions of the first lowest excited state were determined for HOMO → LUMO and HOMO-1 → LUMO+1 transitions (352.26 nm, Fig. S10b,c), which indicated intramolecular charge transfer (ICT) transition from the phenol moieties to the oxalamide one. For **1**-Al^{3+} complex, the first lowest excited state transition, HOMO-4 → LUMO, was forbidden. Therefore, radiative-allowed transition was determined for the second lowest

View Article Online
DOI: 10.1039/C6NJ01544A

excited state, HOMO → LUMO+1 transition, which indicated intramolecular charge transfer (ICT) transition of **1** (368.39 nm, Fig. S11b,c). As shown in Fig S12, there were no obvious changes in the electronic transitions between **1** and **1**-Al^{3+} complex. Only, the hypochromic shift (352.26 to 368.40 nm) was observed upon chelating of **1** with Al^{3+}. These results suggested that the sensing mechanism of **1** toward Al^{3+} was originated from the rigid structure of **1**-Al^{3+} complex, which might inhibit the non-radiative process. Thus, the CHEF effect plays an important role in the fluorescence enhancement.

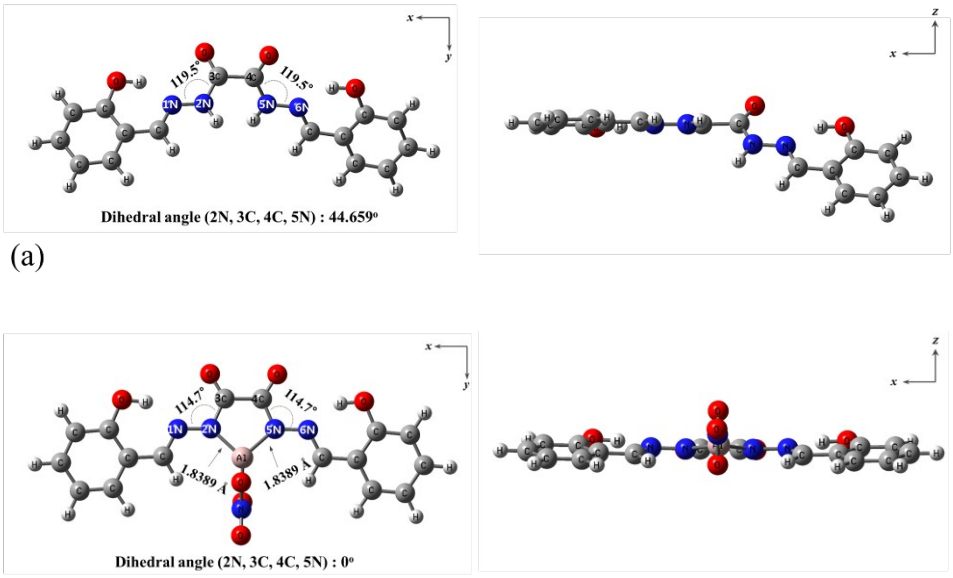

Fig. 5 Energy-minimized structures of (a) **1** and (b) **1**-Al^{3+} from B3LYP level.

3.2 Fluorescence and absorption studies of 1 toward CN^-

We also investigated the fluorescence selectivity of **1** toward different anions (OAc^-, F^-, Cl^-, Br^-, I^-, $H_2PO_4^-$, BzO^-, N_3^-, SCN^-, HS^- and CN^-) in buffer-DMSO (1:1, v/v) solution (Fig. 6). Upon the addition of 72 equiv of each anion to **1**, only CN^- resulted in a drastic enhancement of the emission intensity ($\Phi = 3.41\times10^{-2}$) at 522 nm with excitation at 377

View Article Online
DOI: 10.1039/C6NJ01544A

nm, while other anions showed no or slight change of the fluorescence spectra as compared with the fluorescence ($\Phi = 2.48\times10^{-3}$) of the pure receptor **1**.

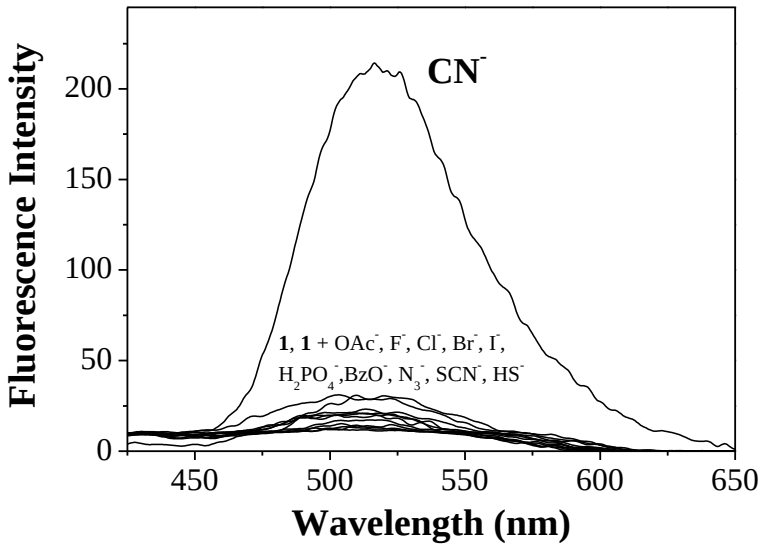

Fig. 6 Fluorescence spectral changes of **1** (30 μM) in the presence of different anions (72 equiv) such as OAc^-, F^-, Cl^-, Br^-, I^-, $H_2PO_4^-$, BzO^-, N_3^-, SCN^-, HS^- and CN^- with an excitation of 377 nm in buffer-DMSO (1:1, v/v) solution.

The recognition ability of **1** for CN^- was investigated by fluorescence titration experiment (Fig. 7). The emission intensity of **1** at 525 nm steadily increased until the amount of CN^- reached 72 equiv. The photophysical properties of **1** were examined by UV-vis titration experiment (Fig. 8). UV-vis spectrum of **1** showed absorption bands at 294 nm and 340 nm. Upon the addition of CN^- to a solution of **1**, the absorption bands have red-shifted to 400 nm, accompanied by the formation of an isosbestic point at 360 nm. These results suggest that only one product was generated from **1** upon binding to CN^-.

View Article Online
DOI: 10.1039/C6NJ01544A

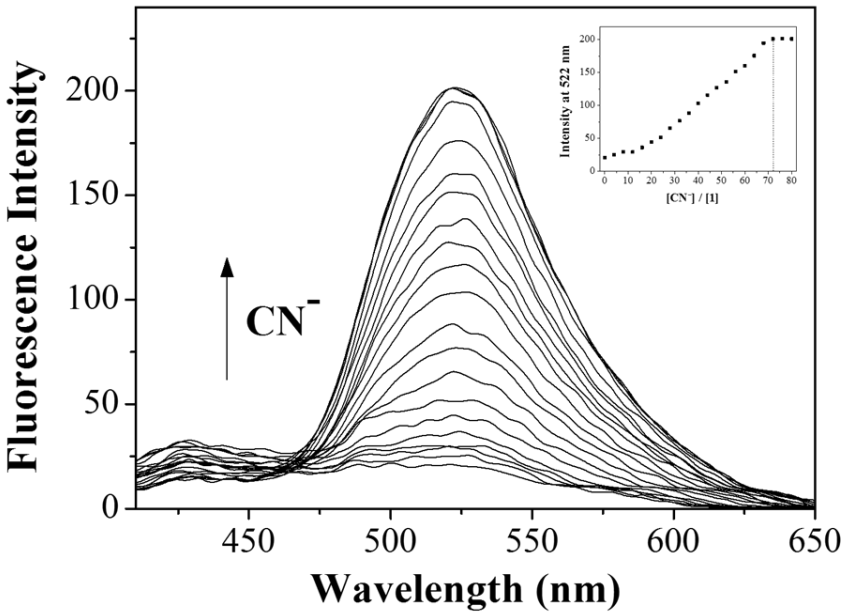

Fig. 7 Fluorescence spectral changes of **1** (30 μM) in the presence of different concentrations of CN^- in buffer-DMSO (1:1, v/v) solution. Inset: intensity (at 522 nm) of **1** as a function of CN^- equiv.

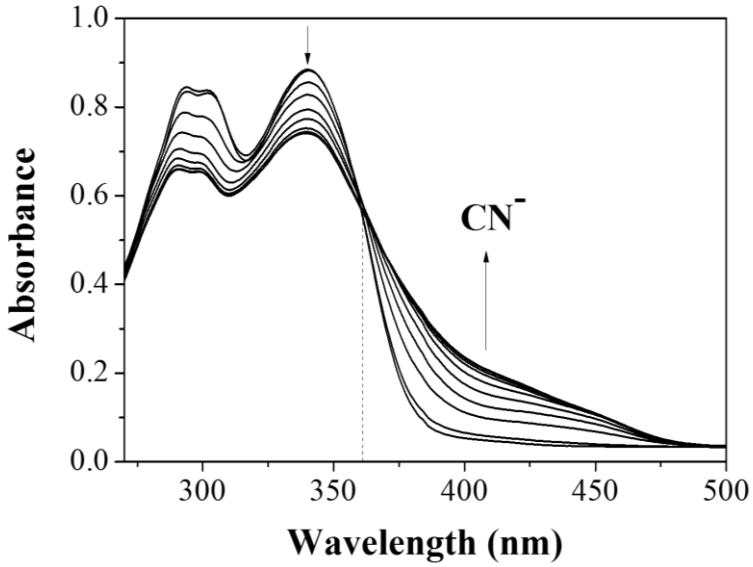

View Article Online
DOI: 10.1039/C6NJ01544A

Fig. 8 UV-vis spectral changes of **1** (30 μM) in the presence of different concentrations of CN^- in buffer-DMSO (1:1, v/v) solution.

The Job plot[73] referred to a 1:1 complexation stoichiometry between **1** and CN^- (Fig. S13), which was further confirmed by ESI-mass spectrometry analysis (Fig. S14). The negative-ion mass spectrum indicated that the first major peak at m/z = 325.10 was assignable to **1**-H^+ [calcd, m/z: 325.09], and the second major peak at m/z = 388.10 was assignable to **1**-$2H^+$ + CH_3CN + Na^+ [calcd, m/z: 388.10]. From the fluorescence titration, the association constant (*K*) of the **1**-CN^- was determined as 2.6×10^2 M^{-1} from Benesi-Hildebrand equation (Fig. S15). The detection limit[74] of receptor **1** as a fluorescence sensor for the analysis of CN^- ions was found to be 27.2 μM (Fig. S16).

The preferential selectivity of **1** as a fluorescent sensor for CN^- was studied in the presence of various competing anions (Fig. 9). For inhibition studies, **1** was treated with 80 equiv of CN^- in the presence of other anions (OAc^-, F^-, Cl^-, Br^-, I^-, BzO^-, N_3^-, SCN^-, $H_2PO_4^-$ and HS^-). It showed no interference in the detection of CN^-. Thus, **1** could be used as a selective fluorescent chemosensor for CN^- in the presence of the competing anions. On the other hand, to further check the preferential selectivity of **1** toward CN^- in the presence of Al^{3+}, the competitive study was carried out in buffer-DMSO (1:1, v/v) solution. As shown in Fig. S17, Al^{3+} interfered with the detection of CN^- under the condition. However, the addition of EDTA (ethylenediaminetetraacetic acid) into a mixture solution of Al^{3+} and CN^- recovered the sensing ability of **1** toward CN^- (Fig. 17).

To examine the practical application of **1** in a variety of pH environments, the pH effect test was conducted in the pH range of 2 to 11 (Fig. S18). The fluorescent sensing ability of **1** toward CN^- remained between pH 7 and 10, which includes the environmentally relevant range of pH 7.0-8.4.[82,83]

View Article Online
DOI: 10.1039/C6NJ01544A

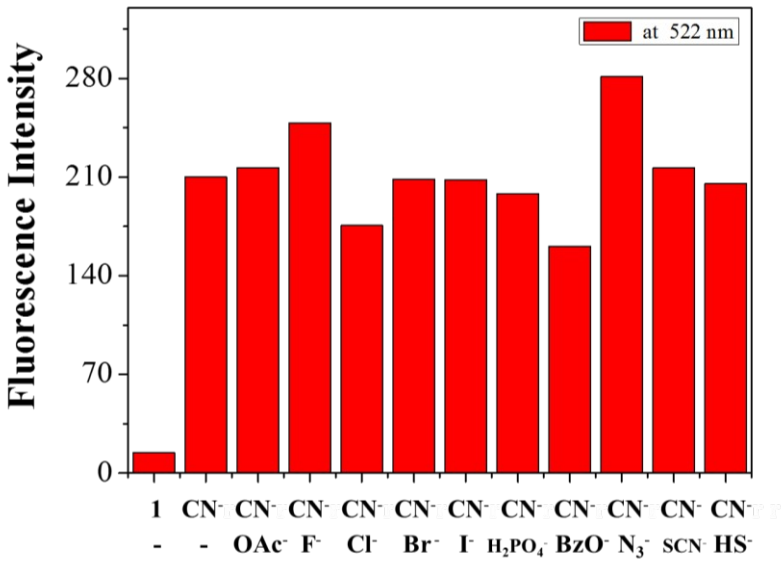

Fig. 9 Competitive selectivity of **1** (30 μM) toward CN^- (72 equiv) in the presence of other anions (72 equiv) with an excitation of 377 nm in buffer-DMSO (1:1, v/v) solution.

To understand the binding interaction between sensor **1** and CN^-, ^1H NMR study was initiated (Fig. 10). Upon addition of 0.5 equiv of TEACN, the protons H_1 (-NH) disappeared. These results indicate that the amine protons might interact strongly with the cyanide through the hydrogen bond. The proton H_7 (-OH) shifted from 12.6 ppm to 11.4 ppm (< 2.0 equiv) and gradually disappeared (2.0 equiv). Meanwhile, the aromatic protons ($H_{3,4,5,6}$) and the imine protons shifted to upfield. On further addition of CN^- (> 2.0 equiv), no shift in the position of proton signals was observed.

View Article Online
DOI: 10.1039/C6NJ01544A

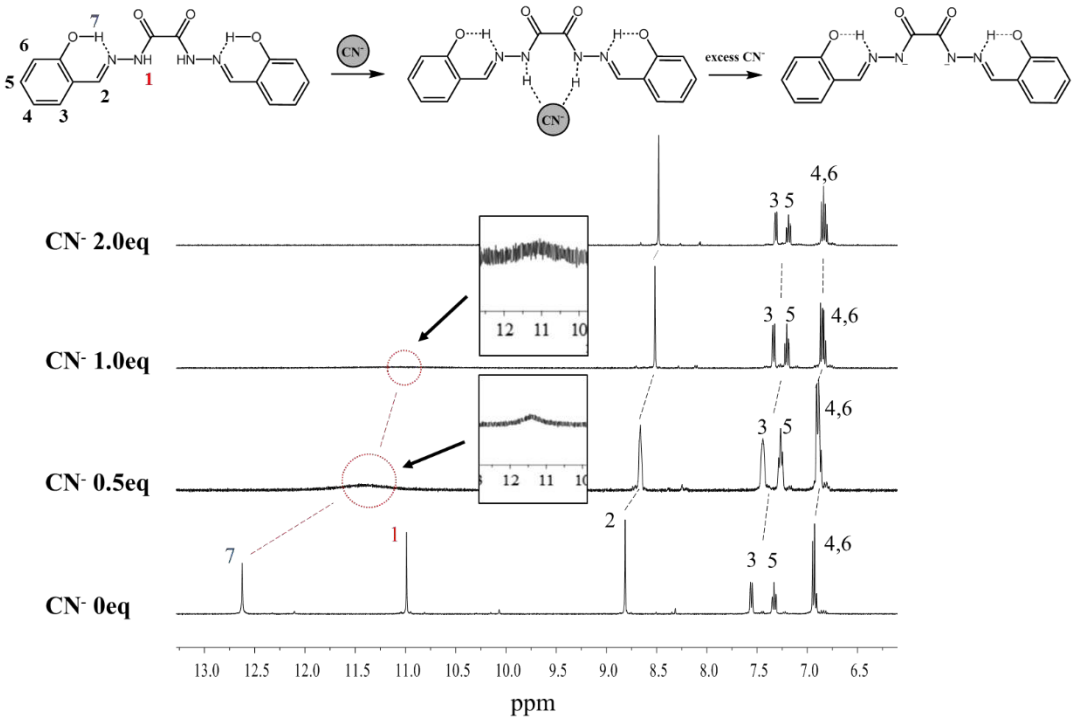

Fig. 10 ^{1}H NMR titration of receptor **1** with CN^{-}.

To clearly demonstrate the fluorescent sensing mechanism of **1** toward CN^{-}, theoretical calculations were performed for **1** and **1**-CN^{-} by applying the B3LYP/6-31g** with CPCM/DMSO. As shown in Fig. S17, the energy-minimized structure of **1** showed a distorted structure with the dihedral angle of 4N, 5C, 6C, 7N = 44.788º and the distances of 1O-2H and 10O-9H are 1.017 Å, respectively (Fig. S19a). **1**-CN^{-} has a planar structure with the dihedral angle of 4N, 5C, 6C, 7N = 0.237º and the distances of 1O-2H and 10O-9H are 1.038 Å, respectively (Fig. 19b). The singlet excitations of **1** and **1**-CN^{-} were investigated by TD-DFT methods (B3LYP/6-31G**/DMSO), and the calculation data were well consistent with the experimental data (Fig. S20a and Fig. S21a). In case of **1**, the main molecular orbital (MO) contributions of the first lowest excited state were determined for

View Article Online
DOI: 10.1039/C6NJ01544A

HOMO → LUMO and HOMO-1 → LUMO+1 transitions (352.74 nm, Fig. S20b,c), which indicated intramolecular charge transfer (ICT) transition from the phenol moieties to the oxalamide one. For **1**-CN^-, the main molecular orbital (MO) contribution of the first lowest excited state was determined for HOMO → LUMO transition (369.69 nm, Fig. S21b,c), which indicated intramolecular charge transfer (ICT) transition. As shown in Fig. S22, there were no obvious changes in the electronic transitions between **1** and **1**-CN^-. However, the energy gap between the HOMO and LUMO of the **1**-CN^- is smaller than that of **1**, which is in good agreement with the bathochromic shift in the absorption observed upon the interaction of **1** with CN^-. Moreover, the fluorescence enhancement from **1** to **1**-CN^- is due to the presence of intramolecular hydrogen boding between **1** and CN^- which induces rigidity into the system (dihedral angles: 44.788° for **1** and 0.237° for **1**-CN^-) and decreases non-radiative decay processes.[84,85] These results suggest that the sensing mechanism of CN^- by **1** might occur by the hydrogen bond pathway. Based on Job plot, ESI-mass spectrometry analysis, ^{1}H NMR titration and theoretical calculations, we propose the sensing mechanism of CN^- by **1** (Scheme 3).

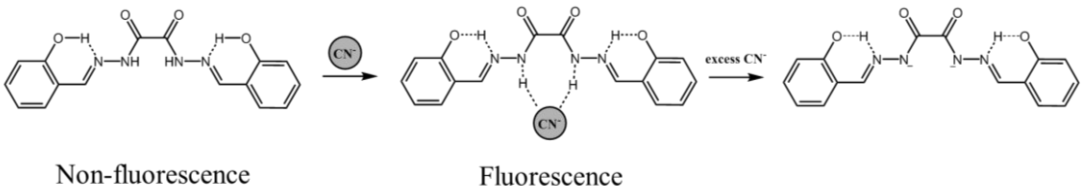

Scheme 3. Proposed sensing mechanism of CN^- by **1**.

4. Conclusion

We have designed and synthesized a simple fluorescent chemosensor **1** that could recognize both Al^{3+} and CN^- in aqueous solution. Al^{3+} induced a significant fluorescence enhancement of **1** while other metal ions showed no obvious change in the spectra. In

View Article Online
DOI: 10.1039/C6NJ01544A

particular, In^{3+} and Ga^{3+} hardly inhibited the fluorescence intensity of the **1**-Al^{3+} complex, whereas it has been a challenge to distinguish Al^{3+} from In^{3+} and Ga^{3+} due to their similar properties. The fluorescence enhancement of **1** with Al^{3+} could be explained by effect of CHEF with theoretical calculations. Moreover, **1** could successfully monitor Al^{3+} in real water samples and living cells. Furthermore, **1** showed a highly selective fluorescence enhancement toward CN^- in the presence of other anions without any interference. The fluorescence sensing of CN^- by **1** was proposed to occur through the hydrogen bonding between **1** and CN^-, which was also supported by TD-DFT studies. On the basis of the results, we believe that receptor **1** will offer an important guidance to the development of single receptors for recognizing both cations and anions.

Acknowledgements

Basic Science Research Program through the National Research Foundation of Korea (NRF) funded by the Ministry of Education, Science and Technology (NRF-2014R1A2A1A11051794, NRF-2015R1A2A2A09001301, and NRF-2014S1A2A2028270) are gratefully acknowledged.

Supplementary Information

Supplementary material associated with this article can be found, in the online version.

View Article Online
DOI: 10.1039/C6NJ01544A

References

1. D. Chen, R. J. Letcher, L. T. Gauthier, S. G. Chu, R. McCrindle and D. Potter, *Environ. Sci. Technol.*, 2011, **45**, 9523-9530.

2. M. W. Hentze, M. U. Muckenthaler and N. C. Andrews, *Cell*, 2004, **117**, 285-297.

3. M. L. Lo Faro, B. Fox, J. L. Whatmore, P. G. Winyard and M. Whiteman, *Nitric Oxide*, 2014, **41**, 38-47.

4. G. K. Kolluru, X. Shen and C. G. Kevil, *Redox Bio*l., 2013, **1**, 313-318.

5. T. Kawano, T. Kadono, T. Furuichi, S. Muto and F. Lapeyrie, *Biochem. Biophys. Res. Commun.*, 2003, **308**, 35-42.

6. S. J. Dixon and B. R. Stockwell, *Nat. Chem. Biol.*, 2014, **10**, 9-17.

7. D. B. Kell, *BMC Med. Genomics*, 2009, **2**, 2.

8. L. Li, P. Rose and P. K. Moore, *Annu. Rev. Pharmacol. Toxicol.*, 2011, **51**, 169-187.

9. A. K. Singh, V. K. Gupta and B. Gupta, *Anal. Chim. Acta*, 2007, **585**, 171-178.

10. D. Astruc, E. Boisselier and C. Ornelas, *Chem. Rev.*, 2010, **110**, 1857-1959.

11. K. P. Carter, A. M. Young and A. E. Palmer, *Chem. Rev.*, 2014, **114**, 4564-4601.

12. D. W. Domaille, E. L. Que and C. J. Chang, *Nat. Chem. Biol.*, 2008, **4**, 168-175.

13. E. Delhaize and P. R. Ryan, *Plant Physiol.*, 1995, **107**, 315-332.

14. D. L. Godbold and E. Fitz, Proc. Natl. Acad. *Sci. U. S. A.*, 1988, **85**, 3888–3892.

15. Y. S. Kim, G. J. Park, J. J. Lee, S. Y. Lee, S. Y. Lee and C. Kim, *RSC Adv.*, 2015, **5**, 11229-11239

16. A. Sahana, A. Banerjee, S. Lohar, A. Banik, S. K. Mukhopadhyay, D. A. Safin, M. G. Babashkina, M. Bolte, Y. Garcia and D. Das, *Dalton Trans.*, 2013, **42**, 13311-13314.

17. T. P. Flaten, *Brain Res. Bull.*, 2001, **55**, 187.

18. P. Nayak, *Environ. Res.*, 2002, **89**, 101.

View Article Online
DOI: 10.1039/C6NJ01544A

19. G. Berthon, *Coord. Chem. Rev*., 2002, **228**, 319.

20. T. Han, X. Feng, B. Tong, J. Shi, L. Chen, J. Zhi and Y. Dong, *Chem. Commun.*, 2012, **48**, 416-418.

21. S. Goswami, S. Paul and A. Manna, *RSC. Adv*., 2013, **3**, 10639-10643.

22. S. Goswami, A. Manna, S. Paul, K. Aich, A. K. Das and S. Chakraborty, *Dalton Trans*., 2013, **42**, 8078-8085.

23. S. Goswami, A. Manna, S. Paul, A. K. Maity, P. Saha, C. K. Quah and H-K. Fun, *RSC. Adv.*, 2014, **4**, 34572-34576.

24. S. Goswami, A. K. Das, K. Aich, A. Manna, H-K Fun and C. K. Quah, Supramolecular Chemistry, 2014, **26**, 94-104.

25. D. Maity and T. Govindaraju, *Inorg. Chem.*, 2010, **49**, 7229-7231.

26. D. Maity and T. Govindaraju, *Chem. Commun.*, 2012, **48**, 1039-1041

27. L. Peng, M. Wang, G. Zhang, D. Zhang and D. Zhu, *Org. Lett.*, 2009, **11**, 1943-6.

28. S. Vallejos, P. Estevez, F. C. Garcia, F. Serna, J. L. de la Pena and J. M. Garcia, *Chem. Commun.*, 2010, **46**, 7951-7953

29. Z. Xu, X. Chen, H.N. Kim and J. Yoon, *Chem. Soc. Rev.*, 2010, **39**, 127-137.

30. J. Kang, E.J. Song, H. Kim, Y. Kim, Y. Kim, S. Kim and C. Kim, *Tetrahedron Lett.*, 2013, **54**, 1015-1019.

31. G. R. You, G. J. Park, J. J. Lee and C. Kim, *Dalton Trans.*, 2015, **44**, 9120-9129.

32. H. Y. Jo, G. J. Park, Y. J. Na, Y. W. Choi, G. R. You, C. Kim, *Dyes and Pigments*, 2014, **109**, 127-134.

33. J. L. Way, *Annu. Rev. Pharmacol. Toxicol.*, 1984, **24**, 451-481.

34. R. A. Anderson and W. A. Harland, *Med. Sci. Law*, 1982, **22**, 35-40.

35. X. Lou, J. Qin and Z. Li, *Analyst*, 2009, **134**, 2071-2075.

View Article Online
DOI: 10.1039/C6NJ01544A

36. C. Young, L. Tidwell and C. Anderson, *Cyanide: Social, Industrial, and Economic Aspects, Minerals, Metals, and Materials Society, Warrendale*, 2001.

37. G. C. Miller and C. A. Pritsos, *Cyanide: Soc., Ind. Econ. Aspects, Proc. Symp. Annu. Meet, TMS,* 2001, 73-81

38. A. Hamza, A.S. Bashammakh, A.A. Al-Sibaai, H. M. Al-Saidi and M. S. El-Shahawi, *Analytica Chimica Acta,* 2010, **657**, 69-74

39. S. Goswami, S. Paul and A. Manna, *Tetrahedron Lett.,* 2014, **55**, 3946-3949.

40. S. Goswami, A. Manna, S. Paul, A. K. Das, K. Aich and P. K. Nandi, *Chem. Comm.*, 2013, **49**. 2912-2914.

41. S. Goswami, S. Paul and A. Manna, *Dalton Trans*., 2013, **42**, 10682-10686.

42. S. Goswami, A. Manna, S. Paul, K. Aich, A. K. Das and S. Chakraborty, *Tetrahedron Lett.,* 2013, **54**, 1785-1789

43. A. P. de Silva, H. Q. Gunaratne, T. Gunnlaugsson, A. J. Huxley, C. P. McCoy, J. T. Rademacher and T. E. Rice, *Chem. Rev.*, 1997, **97**, 1515-1566.

44. T. Ueno and T. Nagano, *Nat. Methods*, 2011, **8**, 642-645.

45. J. J. Lee, S. Y. Lee, K. H. Bok and C. Kim, *J. Fluoresc.*, 2015, **25**, 1449-1459.

46. R. Martinez-Manez and F. Sancenon, *Chem. Rev.,* 2003, **103**, 4419-4476

47. S. Y. Chung, S. W. Nam, J. Lim, S. Park and J. Yoon, *Chem. Commun.*, 2009, **20**, 2866-2868.

48. D. H. Kim, Y. S. Im, H. Kim and C. Kim, *Inorg. Chem. Commun.*, 2014, **45**, 15-19.

49. N. M. Mattiwala, R. Kamal and S. K. Sahoo, *Res. Chem. Intermed.,* 2015, **41**, 391-400.

50. S. A. Lee, G. R. You, Y. W. Choi, H. Y. Jo, A. R. Kim, I. Noh, S. Kim, Y. Kim and C. Kim, *Dalton Trans.,* 2014, **43**, 6650-6659.

51. G. Men, C. Chen, S. Zhang, C. Liang, Y. Wang, M. Deng, H. Shang and B. Y, S.

View Article Online
DOI: 10.1039/C6NJ01544A

Jiang, *Dalton Trans.*, 2015, **44**, 2755-2762.

52. Y. J. Na, Y. W. Choi, J. Y. Yun, K. M. Park, P. S. Chang and C. Kim, *Spectrochim. Acta Part A*, 2014, **136**, 1649-1657

53. D. Maity and T. Govindaraju, *Chem. Eur. J*. 2011, **17**, 1410-1414

54. D. Maity and T. Govindaraju, *Eur. J. Inorg. Chem*, 2011, 5479-5485

55. A. Spath and B. Konig, *Beilstein J. Org. Chem.*, 2010, **6**, 32

56. L. Zhao, D. Sui, J. Chai, Y. Wang and S. Jiang, *J. Phys. Chem. B*, 2006, **110**, 24299-24304.

57. L. Zhao, S. Wang, Y. Wu, Q. Hou, Y. Wang and S. Jiang, *J. Phys. Chem. C,* 2007, **111**, 18387-18391.

58. Y. J. Na, G. J. Park, H. Y. Jo, S. A. Lee and C. Kim, *New J. Chem.*, 2014, **38**, 5769-5776.

59. G. R. You, G. J. Park, S. A. Lee, Y. W. Choi, Y. S. Kim, J. J. Lee and C. Kim, *Sens. Act. B*, 2014, **202**, 645-655.

60. J. J. Lee, G. J. Park, Y. W. Choi, G. R. You, Y. S. Kim, S. Y. Lee and C. Kim, *Sens. Act. B*, 2015, **207**, 123-132.

61. M. J. Frisch, G. W. Trucks, H. B. Schlegel, G. E. Scuseria, M. A. Robb, J. R. Cheeseman, J. A. Montgomery, Jr., T. Vreven, K. N. Kudin, J. C. Burant, J. M. Millam, S. S. Iyengar, J. Tomasi, V. Barone, B. Mennucci, M. Cossi, G. Scalmani, N. Rega, G. A. Petersson, H. Nakatsuji, M. Hada, M. Ehara, K. Toyota, R. Fukuda, J. Hasegawa, M. Ishida, T. Nakajima, Y. Honda, O. Kitao, H. Nakai, M. Klene, X. Li, J. E. Knox, H. P. Hratchian, J. B. Cross, V. Bakken, C. Adamo, J. Jaramillo, R. Gomperts, R. E. Stratmann, O. Yazyev, A. J. Austin, R. Cammi, C. Pomelli, J. W. Ochterski, P. Y. Ayala, K. Morokuma, G. A. Voth, P. Salvador, J. J. Dannenberg, V. G. Zakrzewski, S. Dapprich, A. D. Daniels, M. C. Strain, O. Farkas, D. K. Malick, A. D. Rabuck, K. Raghavachari, J. B. Foresman, J. V. Ortiz, Q. Cui, A. G. Baboul, S. Clifford, J. Cioslowski, B. B. Stefanov, G. Liu, A. Liashenko, P. Piskorz, I. Komaromi, R. L. Martin, D. J. Fox, T. Keith, M. A. Al-Laham,

View Article Online
DOI: 10.1039/C6NJ01544A

C. Y. Peng, A. Nanayakkara, M. Challacombe, P. M. W. Gill, B. Johnson, W. Chen, M. W. Wong, C. Gonzalez and J. A. Pople, *Gaussian 03, Revision D.01, Gaussian, Inc., Wallingford CT,* 2004.

62. A. D. Becke, *J. Chem. Phys.,* 1993, **98**, 5648-5652.

63. C. Lee, W. Yang and R. G. Parr, *Phys. Rev. B,* 1988, **37**, 785-789.

64. P. C. Hariharan and J. A. Pople, *Theor. Chim. Acta,* 1973, **28**, 213-222.

65. M. M. Francl, W. J. Petro, W. J. Hehre, J. S. Binkley, M. S. Gordon, D. J. DeFrees and J. A. Pople, *J. Chem. Phys*., 1982, **77**, 3654-3665.

66. V. Barone and M. Cossi, *J. Phys. Chem. A,* 1998, **102**, 1995-2001.

67. M. Cossi and V. Barone, *J. Chem. Phys.*, 2001, **115**, 4708-4717.

68. N. M. O'Boyle, A. L. Tenderholt and K. M. Langner, *J. Comput. Chem.*, 2008, **29**, 839-845.

69. N. C. Lim, J. V. Shuster, M. C. Porto, M. A. Tanudra, L. Yao, H. C. Freake and C. Bruckner, *Inorg. Chem.,* 2005, **45**, 2018-2030.

70. S. Dey, S. Halder, A. Mukherjee, K. Ghosh and P. Roy, *Sens. Act. B,* 2015, **215**, 196-205.

71. J. J. Lee, G. J. Park, Y. S. Kim, H. J. Lee, I. Noh and C. Kim, *Biosens. Bioelectron.*, 2015, **69**, 226-229.

72. S. Goswami, S. Paul and A. Manna, *RSC Adv.,* 2013, **3**, 25079-25085.

73. P. Job, *Ann. Chim.*, 1928, **9**, 113-203.

74. Y. Chang, S. Wu, C. Hu, C. Cho, M. X. Kao and A. Wu, *Inorg. chim. Acta.,* 2015, **432**, 25-32.

75. D. Maity and T. Govindaraju, *Chem. Commun.,* 2010, **46**, 4499-4501.

76. Y. Wang, M. Yu, Y. Yu, Z. Bai, Z. Shen and F. Li, *Tetrahedron Lett.,* 2009, **50**, 6169-6172.

View Article Online
DOI: 10.1039/C6NJ01544A

77. S. H. Kim, H. S. Choi, J. Kim, S. J. Lee, D. T. Quang and J. S. Kim, *Org. Lett.*, 2010, **12**, 560-563.

78. Y. K. Tsui, S. Devaraj and Y. P. Yen, *Sens. Act. B,* 2012, **161**, 510-519.

79. S. Kim, J. Y. Noh, K. Y. Kim, J. H. Kim, H. K. Kang, S. Nam, S. H. Kim, S. Park, C. Kim and J. Kim, *Inorg. Chem.,* 2012, **51**, 3597-3602.

80. H. Xiao, K. Chen, N. Jiang, D. Cui, G. Yin, J. Wang and R. Wang, *Analyst.,* 2014, **139**, 1980-1986.

81. G. J. Park, H. Y. Jo, K. Y. Ryu and C. Kim, *RSC Adv.,* 2014, **4**, 63882-63890.

82. R. M. Harrison, D. P. H. Laxen and S. J. Wilson, *Environ. Sci. Technol.,* 1981, **15**, 1378-1383.

83. G. J. Park, Y. J. Na, H. Y. Jo, S. A. Lee, A. R. Kim, I. Noh and C. Kim, *New J. Chem.,* 2014, **38**, 2587-2594.

84. A. Dvivedi, P. Rajakannu and M. Ravikanth, *Dalton Trans.,* 2015, **44**, 4054-4062.

85. M. Lee, J. H. Moon, K.M.K. Swamy, Y. Jeong, G. Kim, J. Choi, J. Y. Lee and J. Yoon, *Sens. Act. B,* 2012, **199**, 369-376.

View Article Online
DOI: 10.1039/C6NJ01544A

Graphical Abstract

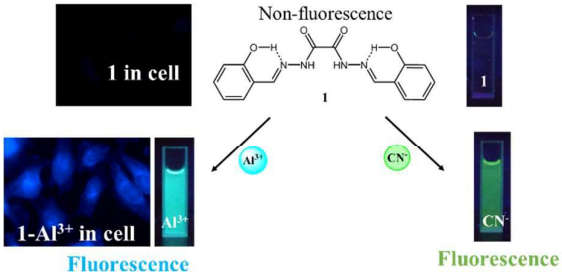

A new turn-on fluorescent chemosensor **1** was developed to detect both Al^{3+} and CN^- and used for a practical and biological application.